Title

Heat content in soil-borehole thermal energy systems in the vadose zone

ISBN

978-1-138-03299-6

Authors

Baser, T
Dong, Y
McCartney, JS

Publication Date

2016

Peer reviewed

Heat Content in Soil-Borehole Thermal Energy Systems in the Vadose Zone

T. Başer
Graduate Research Assistant, University of California San Diego, Department of Structural Engineering, 9500 Gilman Dr. La Jolla, CA 92093-0085, tbaser@ucsd.edu.

Y. Dong
Research Associate, Colorado School of Mines, Coolbaugh Hall Room 336 1012 14th St., Golden, CO 80401, ydong@mines.edu.

J.S. McCartney
Associate Professor, University of California San Diego, Department of Structural Engineering, 9500 Gilman Dr. La Jolla, CA 92093-0085, mccartney@ucsd.edu.

ABSTRACT: This study focuses on understanding the heat content within soil-borehole thermal energy storage (SBTES) systems installed in different types of soils in the vadose zone. Temperature fluctuations in the atmosphere can create a variety of heat flux conditions resulting in different temperature gradients in the subsurface, even when a surficial insulation layer is incorporated. A three-dimensional (3D), transient finite element model was built in COMSOL to consider the representative field conditions as well as coupled heat transfer and water flow processes in the unsaturated soil within the SBTES system. The heat content is used to quantify the heat gain above the temperature profile expected above the ambient ground temperature fluctuations. The heat content changes with different type of soils as the hydraulic and thermal properties are specific to soil types. Results indicate that presence of an insulation layer leads to a significant heat gain in the shallow subsurface in all types of soils.

1 INTRODUCTION

Soil-Borehole Thermal Energy Storage (SBTES) systems are used to store heat collected from renewable sources so that it can be used later for heating of buildings (Sibbitt et al. 2012; Zhang et al. 2012, McCartney et al. 2013, Başer & McCartney 2015). They function in a similar way to conventional geothermal heat exchange (GHE) systems, where heat is transferred from a source to a sink via circulation of fluid through a series of closed-loop heat exchangers. However, they differ from GHE systems in that the heat is injected or extracted continuously over the course of a season into the borehole heat exchanger array. Further, the borehole array in a SBTES system is overlain by a hydraulic barrier to retain pore water within the subsurface and a thermal insulation layer to minimize heat losses to the atmosphere (Başer et al. 2015a, 2015b, 2016).

In the shallow subsurface, below the soil-atmosphere interface, heat transport plays a critical role in determining the energy fluxes between the soil surface and the atmosphere. Atmospheric conditions may be very complex due to the climatic changes and can create a variety of heat flux conditions at the soil surface. In arid and semiarid regions, temperature gradients in the shallow subsurface can be very large and may have a significant effect on temporal temperature distributions.

The main goal of this paper is to understand the impact of the insulation layer on spatial and temporal temperature distributions in heat exchanger arrays installed in different types of soils in unsaturated conditions, considering coupled heat flow and thermally induced water flow. Thus a series of numerical analyses were performed on unsaturated silt and clay soils to evaluate the role of the surficial insulation layer along with the atmospheric boundary conditions. These are compared with preliminary data from a field SBTES site in San Diego, CA.

2 BACKGROUND AND FIELD STUDY

Several field and numerical studies have established that SBTES are proven to be efficient at storing heat in the subsurface (Sibbitt et al. 2012, Zhang et al. 2012, Başer et al. 2015b). However, a better understanding of the heat transfer processes in these systems is required as the temperature increase in the SBTES arrays is highly dependent on the thermal properties of the soils and these properties change with the type of soil and the degree of saturation of the soil. To prevent heat loss from the upper surface of an SBTES system, layers of expanded polystyrene (EPS) are placed atop the array beneath a vegetative soil layer. There have only been a few studies justifying the role of the insulation layer. Başer et al. (2016) performed a numerical study on this topic, but only considered 2D flow processes and did not evaluate the change in temperature above ambient ground temperature fluctuations.

Recently a full-scale SBTES system was installed at the Englekirk Research Center on the University of California San Diego Campus. The SBTES system consists of a vertical borehole array and two horizontal arrays. Borehole array includes 15 m deep 15 borehole heat exchangers in a hexagonal array with a spacing of 1.5 m, as shown in Figure 1. The heat exchangers consist of high density polyethylene tubing with a "U"-shape coupling at the base. Three additional boreholes were installed that included thermistor strings, which have six thermistors along the length of a single cable. Their purpose is to measure the temperature distribution with depth to infer heat transfer processes within the array. One of these thermistor strings was installed in an isolated borehole to observe undisturbed ground temperature fluctuations during operation, which is a useful variable to assess the heat storage in an SBTES array.

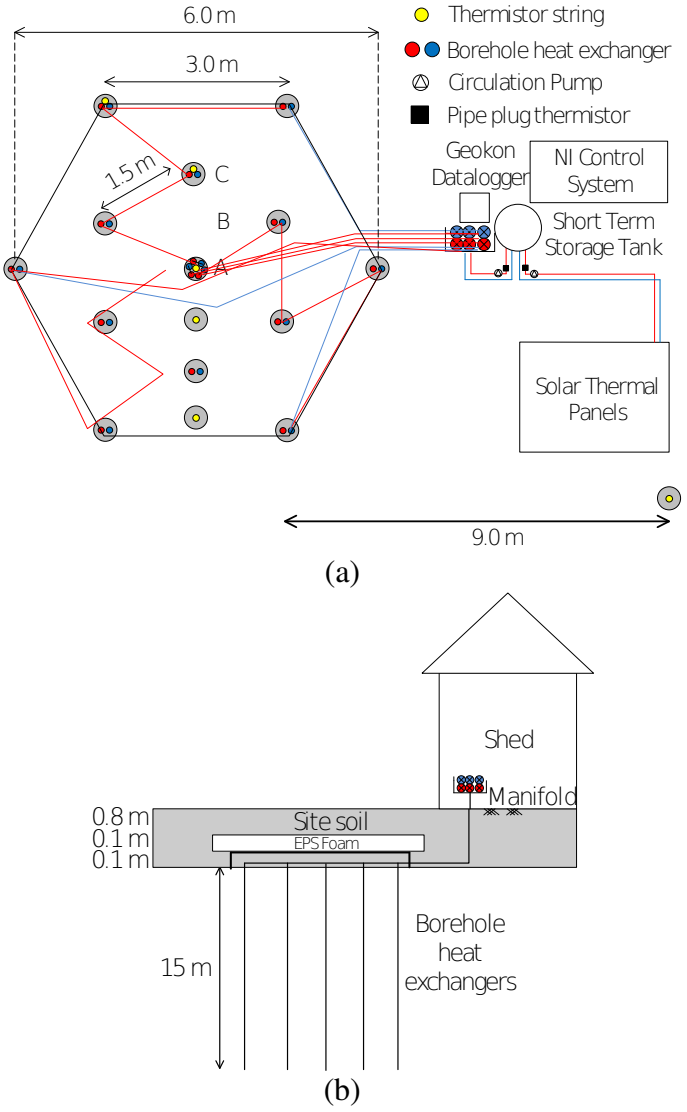

Figure 1. UCSD SBTES system: (a) Plan; (b) Elevation

After drilling the boreholes, the soil excavated to a depth of 1 m around the array. After placing a layer of site soil to cover the heat exchangers, a 30 mil-thick hydraulic barrier was placed on the soil surface. A layer of expanded polystyrene (EPS) insulation was then placed on top of the hydraulic barrier, and the site soil was then backfilled up to grade. Before operation of the system, the initial ground temperature fluctuations are being collected to determine the effect of the ambient air temperature fluctuations on the temperature penetration into the soil under the array and in the undisturbed ground. The ground temperature data collected inside of the array where the array is covered with an insulation layer and outside of the array from September 13, 2015 to February 15, 2016 are plotted in Figure 2. Placing an insulation layer decreases the effect of the ambient temperature fluctuation on the soil temperature.

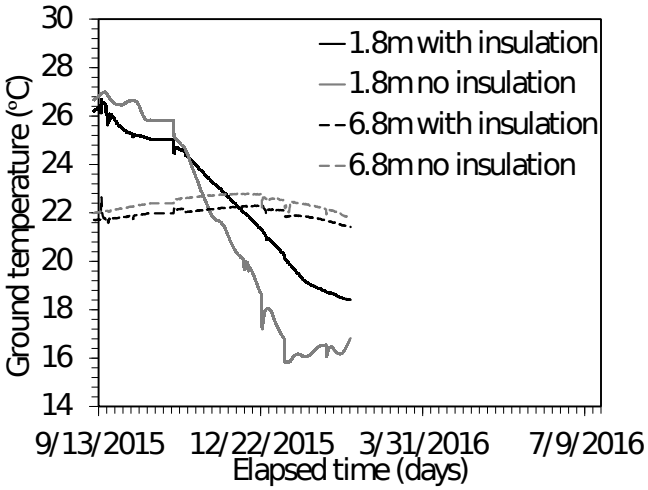

(a)

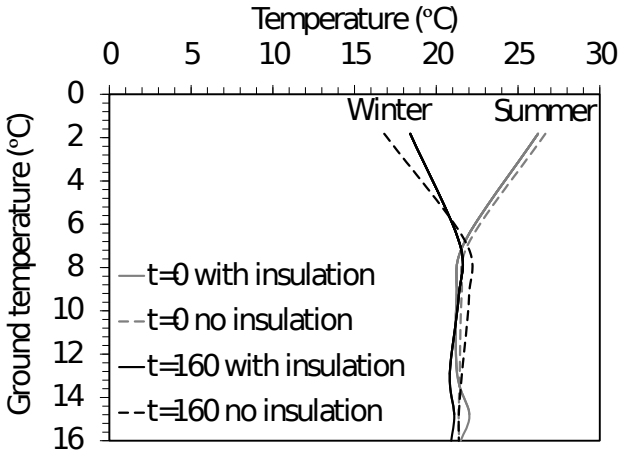

(b)

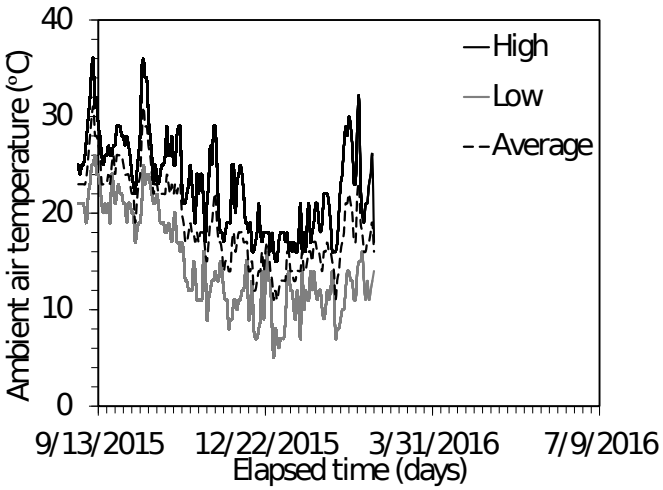

(c)

Figure 2. Initial temperatures of UCSD site with and without insulation layer (a) Time series for different depths; (b) Temperature profiles on February 15, 2016; (c) Ambient air temperature

3 NUMERICAL MODEL

3.1 *Model Formulation*

A transient three-dimensional finite element model was built in COMSOL to predict temperature distributions inside and outside of the thermal heat exchanger arrays. The model was developed considering both heat transfer and water flow since when the unsaturated soils is heated water flows due to the decrease in density. The other driving mechanism for water flow is the alteration of surface tension with temperature. Thermally-induced vapor flow is not considered in this study.

Water flow in unsaturated soils can be expressed by Richards' equation assuming that air pressure in the pores equal to atmospheric pressure. Thus mass balance in unsaturated soils is expressed as follows (Bear 1972):

$$n\frac{dS_w}{dP_c}\frac{\partial \rho_w P_c}{\partial t} + \nabla \cdot \left(\frac{-\rho_w k_{rw} k_{\text{int}}}{\mu_w} (\nabla P_w + \rho_w g) \right) = -Q_m \tag{1}$$

where n = porosity of the soil; S_w = wetting (water) degree of saturation (dim.); ρ_w = density of water (kg/m^3); μ_w = dynamic viscosity of water (Pa·s); P_c = capillary pressure ($P_c = P_{nw}-P_w$) (kPa); t = time (s); k_{int} = intrinsic permeability of soil (m^2); k_{rw} = relative permeability of water (dim.); g = gravitational acceleration (m^2/s); and Q_m= mass source (kg/(m^{3}s)). Since phase change between liquid water and water vapor was neglected in this study, Q_m was assumed to be to zero.

Heat transfer in unsaturated soils is governed by the combined Fourier's and Newton's law. The governing equation for heat transfer is porous media can be expressed as follows:

$$(\rho C_p)\frac{\partial T}{\partial t} + \nabla \cdot (\rho C_p u_w T) = \nabla \cdot (\lambda \nabla T) + Q \tag{2}$$

where ρ = total density of the soil (kg/m^3); C_p = specific heat capacity of the soil at constant pressure (J/(kgK)); u_w = Darcy velocity; T = absolute temperature (K); λ = apparent thermal conductivity of the soil (W/(mK)); and Q = heat source (W/m^3).

3.2 *Model Geometry and Boundary Conditions*

The model geometry consists of an array of 15 m-deep vertical borehole geothermal heat exchangers installed in a deep homogeneous soil layer in an array having a width of 30 m and a depth of 30 m. A 0.1 m-thick insulation layer was placed on top of the heat exchangers, which was covered by a layer of site soil. The details of the model geometry is given in Figure 3. Symmetry was used in configuring the model geometry, with one of the geothermal heat exchangers at the corner of the array, and the other two are spaced at a distance of 2.5 m from the center in orthogonal directions.

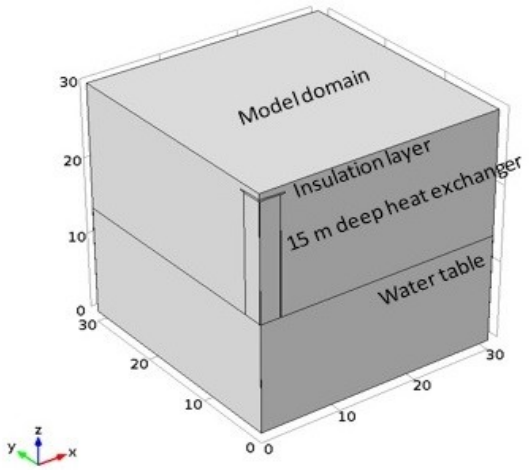

Figure 3. Model geometry

For heat transfer, a constant heat flux of 30 W/m was applied at the borehole boundaries for a period of 90 days. A sinusoidal temperature function was applied at the top assuming that maximum and minimum daily air temperatures are 25°C and 10°C. The bottom temperature was fixed to 12°C because of the groundwater. For water flow, zero flux was assumed for all boundaries except the bottom boundary, where a constant total head of 14 m was applied.

The initial temperature of the domain was assumed to be uniform and equal to 12°C. This is equal to the mean annual air temperature in San Diego, CA, and represents the transition profile between the hot and cold seasons of the year. The water table was assumed to be at a depth of 16 m, coinciding with the bottom of the heat exchangers. The initial conditions for the profiles of degree of saturation and suction with depth correspond to hydrostatic conditions.

The entire domain is assumed to be a uniform and isotropic soil layer. The properties of two soil types were considered for the soil layer, those of Hopi silt and Denver claystone. The thermal and hydraulic properties needed for coupled heat transfer and water flow analyses of these soil are given in Figures 4(a) to 4(d) (Lu and Dong 2015). These properties differ for the different type of soils as they are dependent on the grain size, pore size distribution, and degree of saturation of the soil. Saturated thermal conductivity of Hopi silt and Denver claystone are 5.3×10^{-7} and 2.2×10^{-7} (m/s), respectively.

After the implementation of the initial and boundary conditions, the system of partial differential equations (1) and (2) in three-

dimensional domain was simultaneously solved using the COMSOL Multiphysics software that is based on the finite element method. The simulated domain has a volume about 10 times that of the heat exchanger domain in order to minimize boundary effects. Also initial simulations verified that there was no boundary effects.

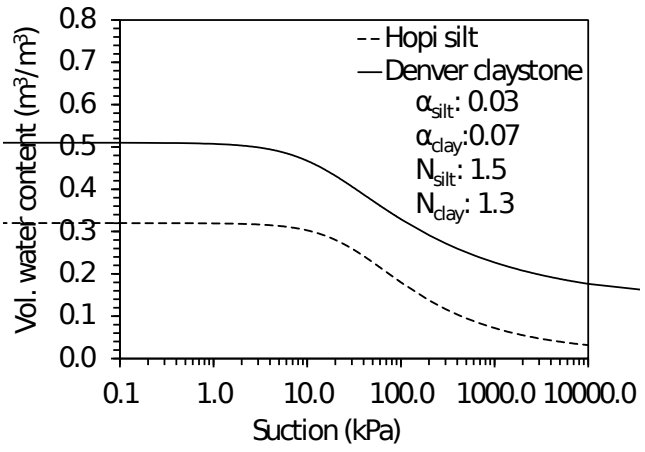

(a)

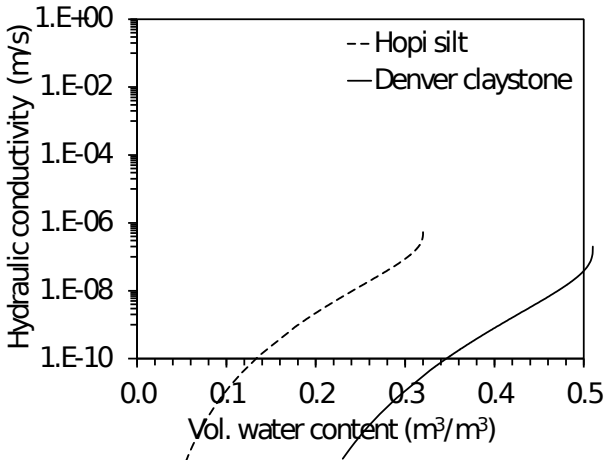

(b)

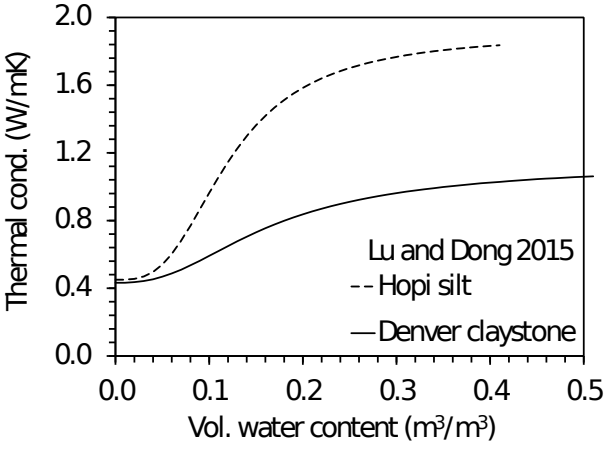

(c)

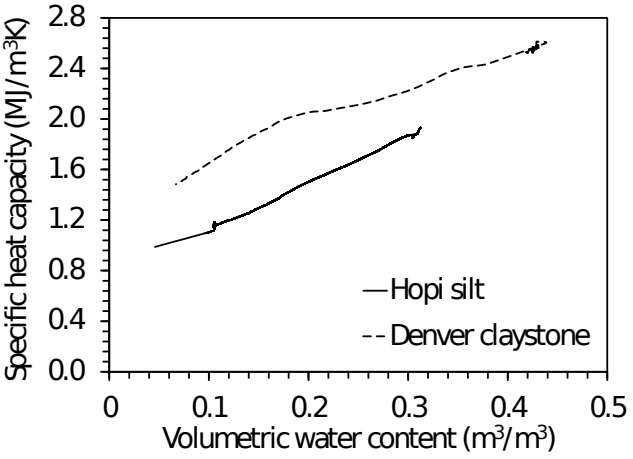

(d)

Figure 4. Hydraulic and thermal properties of soils used in the analyses (a) SWRC; (b) HCF; (c) TCF; (d) C_p vs VWC

4 ANALYSIS

Spatial and temporal distributions of the temperatures inside and outside of the heat exchanger array were determined. In heat transfer modeling efforts surface temperature boundary conditions are important as the ambient air temperatures have an effect up to depth of 10 m from the surface (Brandl 2006). The first analysis was performed to observe the penetration of surface temperature without any heat input into the soil layer. Then, heat input is initiated until the last time step reaches 90 days for two cases; without the insulation layer and with the insulation layer. Temperature profiles inside of the array for Hopi silt were plotted for different time steps at x=1.25 m, y=1.25 m, and are given in Figures 5(a), 5(b), and 5(c).

Ambient temperature fluctuations has an effect on the soil temperature distribution in the subsurface. However, the amplitudes decrease depth with due to the thermal inertia of the soil (Brandl 2006). The penetration depth from the field data is 7 m while it is 11 m from the numerical results. This is mainly because of the different thermal properties of the soils. The baseline temperature distribution trend from numerical analysis is compatible with those of measured in the field as shown in Figure 5a. Also insulation layer in the numerical analysis led to a relatively lower temperature values inside of the array.

A maximum temperature of 43 °C without the insulation layer is observed at 7.5 m at the end of the heating while the temperature reaches a value of 44 °C at a depth of 6 m in the analysis with the insulation as shown in Figures 5b and 5c. Yesiller et al. (2005) defined a new parameter for evaluating exothermic reactions in municipal solid waste landfills called the "heat content". This parameter can be used to account for the amount of heat in the landfill above that expected for seasonal ground

temperature fluctuations at a given depth. In a similar way heat content, HC (°C×day/day) of the heat exchanger array was determined by first calculating the area between the time series curves for the temperature increase by the constant heat input and the baseline temperatures. Then it was divided by the duration of the analysis period to normalize HC with respect to time. HC can be expressed by the following equation:

$$HC = \int_{t=0}^{t=90} (T - T_{base})dt \quad (3)$$

To calculate the area, first the temperature time series at different locations are plotted in Figures 6(a) to 6(c). The maximum temperature inside of the array where is very close to the center borehole was 55°C while it decreased a value of 23°C outside of the array. The insulation layer had a negligible effect on temperature at a depth of 6 m. This effect is the same inside and outside of the array.

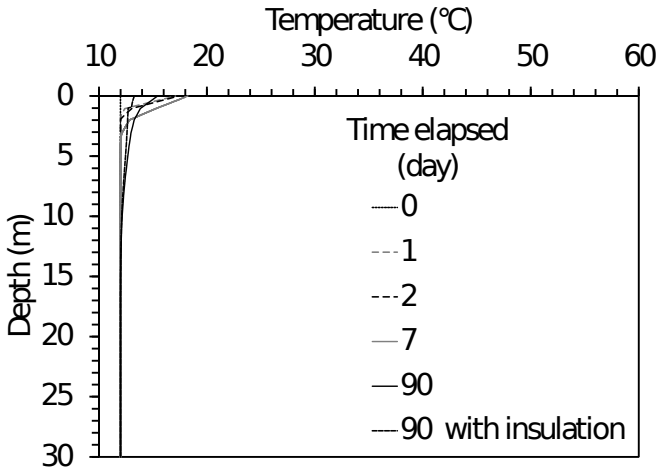

(a)

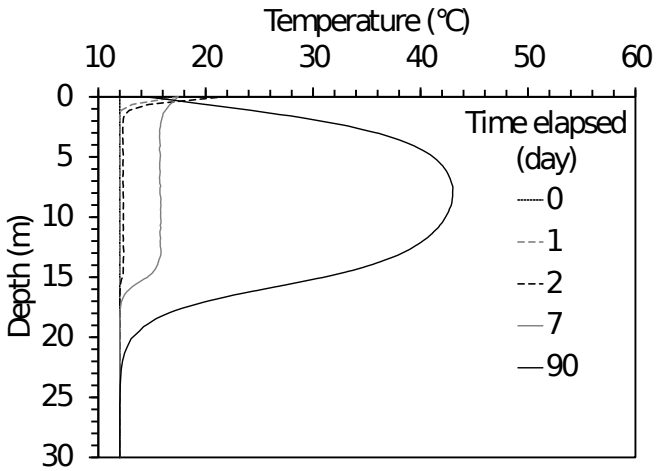

(b)

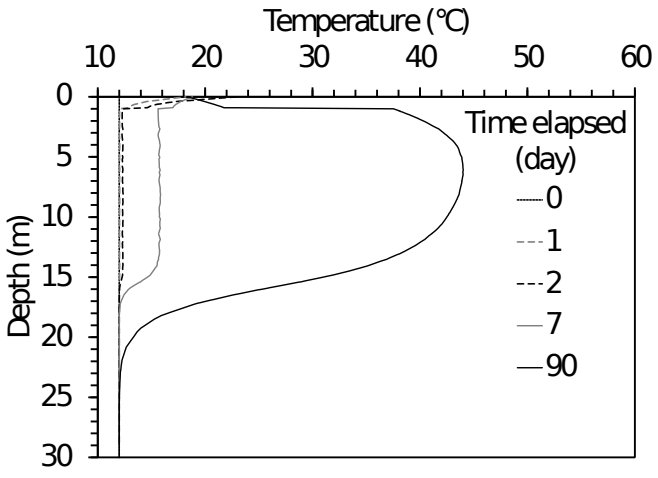

(c)

Figure 5. Temperature profiles inside of the heat exchanger array for Hopi silt (a) Baseline; (b) Heat input without insulation; (c) Heat input with insulation

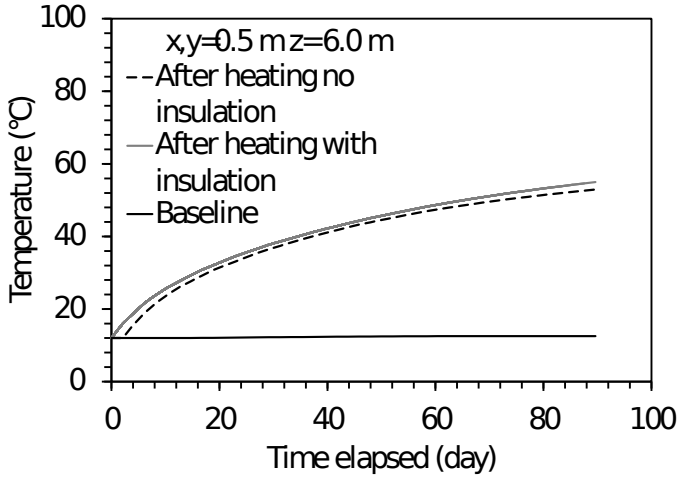

(a)

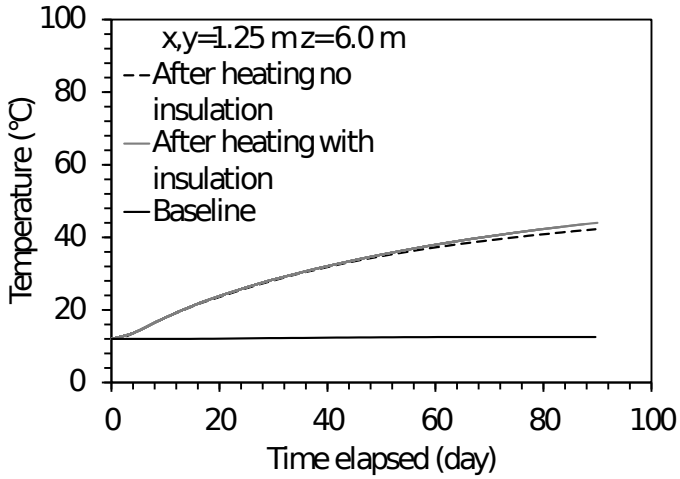

(b)

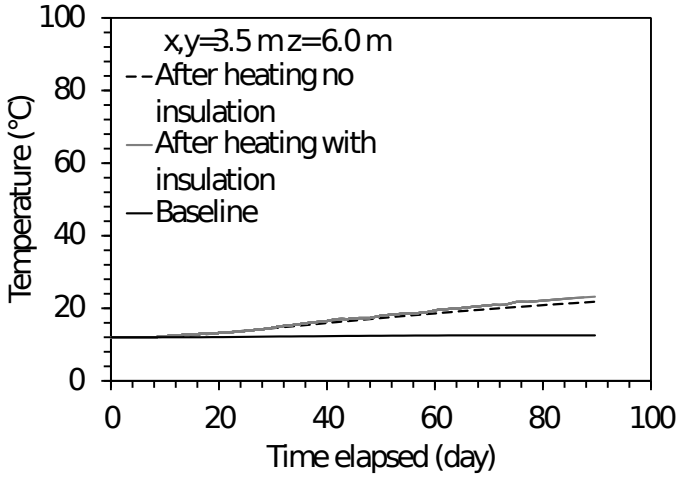

(c)

Figure 6. Temperature time series at a depth of z = 6.0 m: (a) 0.5 m from the center; (b) 1.25 m from the center; (c) 3.5 m from the center

Heat contents for two different depths was calculated and plotted at the different locations (inside and outside of the array) for Hopi silt as shown in Figures 7(a) and 7(b). It was observed that the insulation layer has a greater effect on the heat content of the soil closer to the surface.

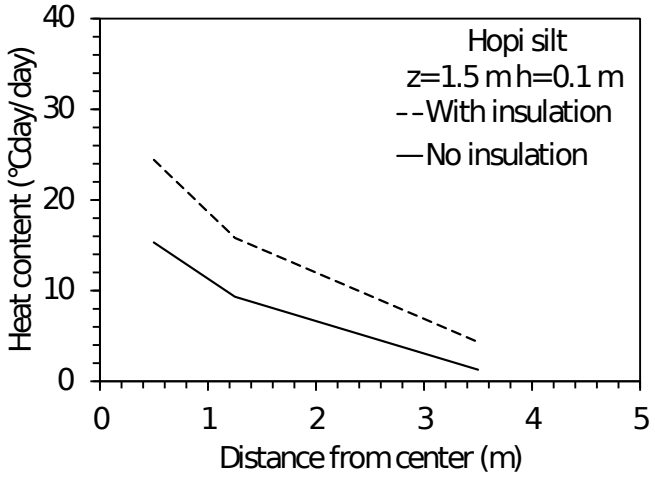

(a)

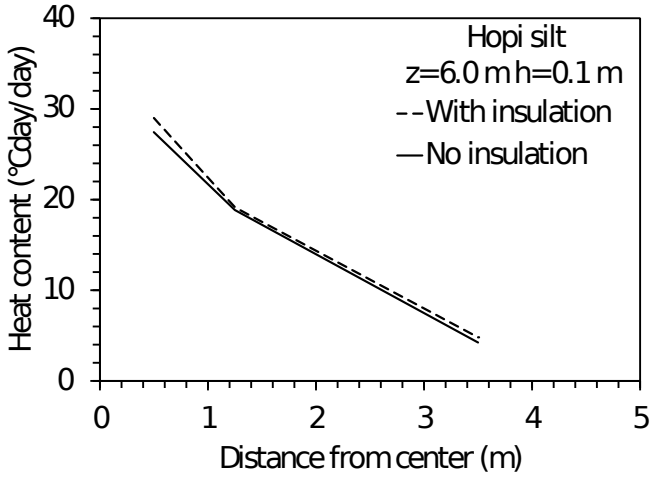

(b)

Figure 7. Heat content changing with distance from the center of the array (a) at a depth of 1.5 m; (b) at a depth of 6.0 m

The heat content must be dependent of soil type as the thermal and hydraulic properties change with different soils. To understand the effect of soil type on the heat content a series of analyses were performed for Denver claystone applying the same boundary conditions. Although not given here, the temperature in the middle of the array reached a temperature value of 51.7°C at the depth of 6.2 m due to the relatively low thermal conductivity. As the insulation layer has its greater effect very close to surface heat contents for Denver claystone are plotted in Figure 8(a) at 1.5 m. The maximum heat content value of 32 (°C×day/day) was observed at 1.5 m. This value is 31% greater than the value of 24.4 which was observed for Hopi silt in Figure 8(b).

The contribution of the insulation layer on heat content was also an interesting subject to investigate. Thus, heat contents were determined for the temperature gain by the insulation layer having different thicknesses (h=0.1m and h=0.2m). This time the area for the temperature increase with insulation layer and the temperature increase without the insulation layer were calculated for different soil types. The contribution of the insulation layer ranges between 60-70% for Hopi sit while this value is 24% for Denver claystone inside of the array. It was also observed that when the thickness of the insulation layer is doubled, the heat content increases in the array while it slightly decreases outside of the array at very close to the surface. This is because with the thicker insulation layer more heat can be preserved inside the array resulting in a lower temperature increase outside of the heat exchanger array. This increase also differs with different type of soils as shown in Figures 9(a) to 9(d). The heat content increase with increasing insulation layer is quantitatively greater in soils having higher thermal conductivity than in soils with a comparatively lower thermal conductivity. There was no significant increase in heat content at a depth of 6 m due to the effect of the insulation layer. This is because the heat at this depth is not affected greatly by the surface temperature fluctuations.

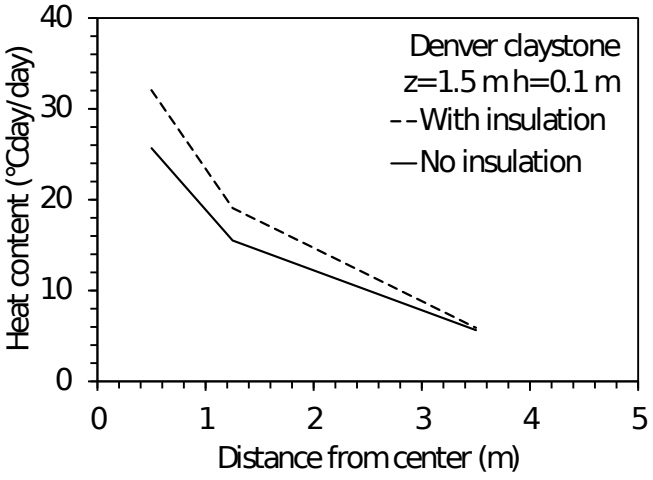

(a)

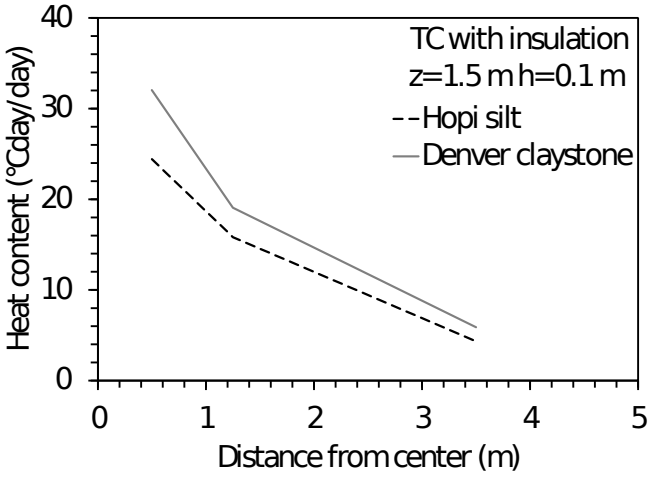

(b)

Figure 8. Heat content versus distance from the center for Denver claystone (a) Denver claystone; (b) Comparison of different soil types

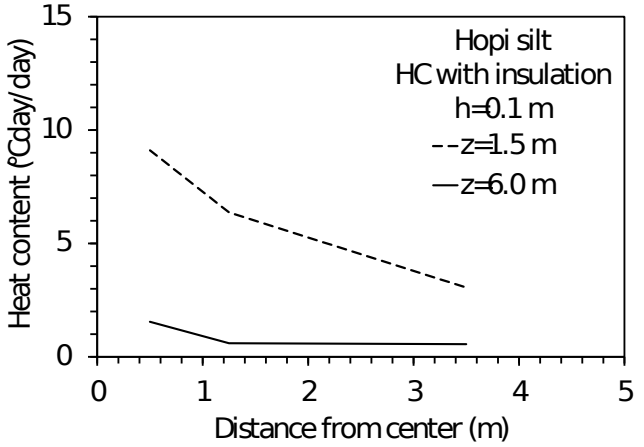

(a)

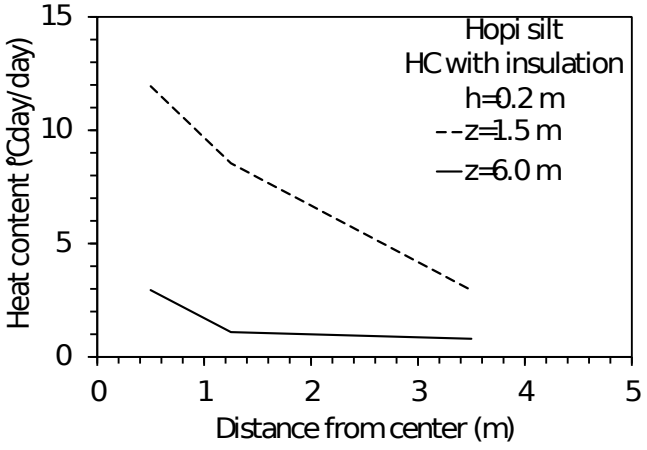

(b)

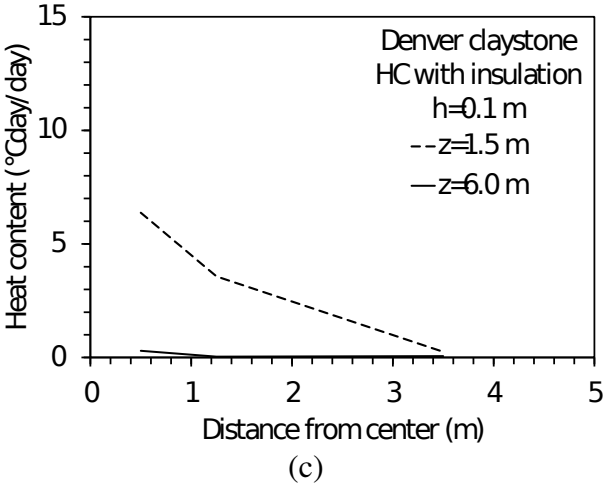

(c)

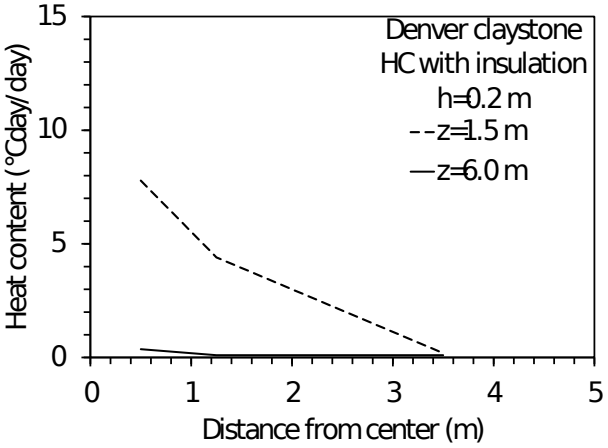

(d)

Figure 9. The effect of insulation layer on the heat content (a) Hopi silt h=0.1 m; (b) Hopi silt h= 0.2 m; (c) Denver claystone h= 0.1 m; (d) Denver claystone h= 0.2 m

Thermally-induced water flow has been studied by many researchers as the thermal properties of soils change with degree of saturation (Philip & deVries 1957, Smits et al. 2012, Başer et al. 2014). The study by Lu and Dong (2015) has shown that there is a significant increase in thermal conductivity as well as specific heat capacity with increasing degree of saturation from dry to unsaturated conditions. Thus in the modeling efforts thermally induced water flow is considered as the water in the pores decrease in density and moves away from heat source to cold regions. This movement is mainly dependent on the hydraulic conductivity of the different soils (Catolico et al. 2016) and the temperature gradients.

To understand the unsaturated water flow in the heat exchanger arrays due to the temperature gradients the initial and final volumetric water content profiles were plotted for Hopi silt in Figure 10. It was seen that even though this movement is small, its contribution to the specific heat capacity is not negligible. The biggest increase in volumetric water content was observed very close to the heat source due to the higher temperature increase while the thermally induced water flux magnitude decreases with increasing distance from the center. It should be noted that this analysis does not consider thermally-induced vapor flow, which may have an

additional effect on the thermally induced water flow. However, this analysis is quite complex and will be left for a future study. The conclusions regarding the role of the insulation layer are still expected to be valid regardless of not considering this additional coupled flow process.

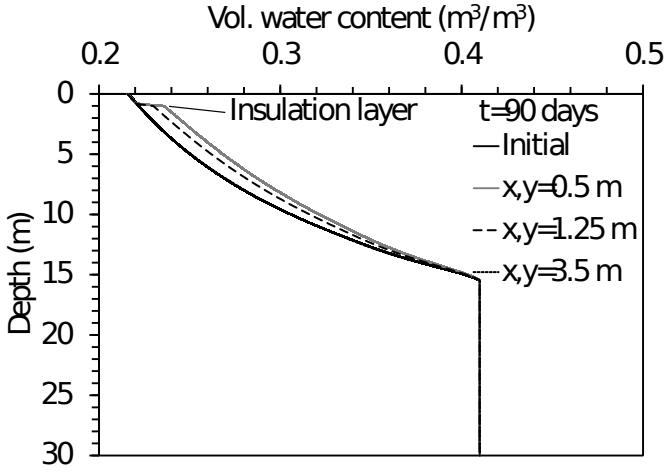

Figure 10. Volumetric water content profiles inside and outside of the array.

5 CONCLUSIONS

This study focuses on numerical simulations of the spatial and temporal temperature distributions in soil-borehole thermal energy storage (SBTES) systems with and without a surficial insulation layer. A 3D transient finite element model was built to consider representative field conditions in an unsaturated soil layer in and around the SBTES system. Experimental and numerical results indicate that installing an insulation layer on top of the heat exchanger array leads an increase in the temperature in the shallow subsurface by reducing the heat exchange between the subsurface and the thermal storage array. The "heat content" of a thermal heat exchanger array defined as the area between the time series curves for the temperature increase by the constant heat input and the baseline temperatures normalized by the time was used to quantify the heat storage in the array. The magnitude of heat content (HC) was observed to increase in the array with increasing depth. Soils having a higher thermal conductivity has a lower HC values as the heat can dissipate faster under high temperature gradients. Increase in temperature with an insulation layer is also quantified with the increase in HC. This increase is bigger in the soils having a relatively higher thermal conductivities. When the insulation layer is doubled the preserved amount of heat in the array increases. This increase is significant right below the surface while there is no significant increase with increasing depth.

Acknowledgements

Funding from National Science Foundation (NSF 1230237) is much appreciated. The opinions are those of the authors alone and do not reflect those of the sponsor.

REFERENCES

Başer, T., Linkowski, D. & McCartney, J.S. 2014. Charging and discharging of soil-borehole thermal energy storage systems in the vadose zone. In: Bouazza, Abdulmalek (Editor); Yuen, Samuel T S (Editor); Brown, Bruce (Editor). 7th International Congress on Environmental Geotechnics: ICEG2014: Engineers Australia, 2014: 362-369.

Başer, T. & McCartney, J.S. 2015a. Development of a full-scale soil-borehole thermal energy storage system. Proc. Int. Foundations Conference and Equipment Exposition (IFCEE 2015). ASCE. pp. 1608-1617.

Başer, T., Lu, N., & McCartney, J.S. 2015b. "Operational response of a soil-borehole thermal energy storage system." ASCE Journal of Geotechnical and Geoenvironmental Engineering. 04015097-1-12. 10.1061/(ASCE)GT.1943-5606.0001432.

Başer, T., McCartney, J.S., Moradi, A., Smits, K., and Lu, N. 2016. "Effect of a thermo-hydraulic insulating layer on the long-term response of soil-borehole thermal energy storage systems." GeoChicago 2016: Sustainability, Energy and the Geoenvironment. Chicago. Aug. 14-18. pp. 1-10.

Bear, J. 1972. Dynamics of Fluids in Porous Media. Dover, Mineola, N. Y., 764 p.

Brandl, H., 2006. Energy foundations and other thermo-active ground structures. Géotechnique 56(2): 81–122.

Catolico, N., Ge, S., & McCartney, J.S. 2016. Numerical modeling of a soilborehole thermal energy storage system. Vadose Zone Hydrology. 1-17.doi:10.2136/vzj2015.05.0078.

Lu, N. & Dong, Y. 2015. A closed form equation for thermal conductivity of unsaturated soils at room temperature. Journal of Geotechnical and Geoenvironmental Eng. 141(6), 04015016.

Philip, J.R. & de Vries, D.A. 1957. Moisture movement in porous materials under temperature gradients. Trans. Amer. Geophys. Union 38:222–232.

Sibbitt, B., McClenahan, D., Djebbara, R., Thornton, J., Wong, B., Carriere, J., & Kokko, J. 2012. The performance of a high solar fraction seasonal storage district heating system – Five years of operation. Energy Procedia, 30: 856-865.

Smits, K.M., Sakaki, S.T., Howington, S.E., Peters, J.F., & Illangasekare, T.H. 2013. Temperature dependence of thermal properties of sands across a wide range of temperatures (30-70°C).VadoseZone Journal, doi:10.2136/vzj2012.0033.

Zhang, R., Lu, N. & Wu, Y. 2012. Efficiency of a community-scale borehole thermal energy storage technique for solar thermal energy. Proc. GeoCongress 2012. ASCE. 4386-4395.

Yesiller, N., Hanson, J.L. & Liu, W-L. 2005. Heat Generation in Municipal Solid Waste Landfills. Journal of Geotechnical and Geoenvironmental Eng. 131(11), 1330-1344.